

Infrared Thermal Field Emitted from Human Body. Thermovision

Ignat Ignatov^{1*} Oleg Mosin² Christos Drossinakis³

1. DSc, professor, Scientific Research Center of Medical Biophysics (SRCMB),
32 N. Kopernik St., Sofia 1111, Bulgaria
2. PhD, Biotechnology Department, Moscow State University of Applied Biotechnology,
33 Talalikhina St., Moscow 109316, Russian Federation
3. Dipl. Eng., IAWG-GmbH, 61A Königsteiner St., Frankfurt, Germany, Chalkida, Greece

* E-mail of the corresponding author: mbioph@dir.bg

Abstract

This paper presents the results of evaluation of possible biophysical methods for registering of infrared thermal field of the human body in the electromagnetic range. Many types of emissions (electromagnetic waves, infrared radiation, thermo radiation, bioluminescence) emitted from the human body were researched. There were shown the results with infrared thermography (IRT) results. Some important physical characteristics were also demonstrated (energy of hydrogen bonds, wetting angle, surface tension) of water by the methods of non-equilibrium energy (NES) and differential non-equilibrium energy (DNES) spectrum of water, that helps understand in general how electromagnetic radiation interacts with water and establishes the structural alterations of water. The spectral ranges of NES and DNES are in middle infrared range.

Keywords: electromagnetic waves, infrared thermal field, NES, DNES

1. Introduction

All living organisms have a cellular, and therefore, a molecular organized structure. The living processes inside them run on a cellular and a molecular level. Bioelectrical activity is one of the very important physical parameters of living organisms (Ignatov et al., 1998). Bioelectric potentials generated by various cells are widely used in medical diagnostics and are recorded as electrocardiogram, electromyogram, electroencephalogram, etc. It was proved that the human body and tissues emanate weak electromagnetic waves, the electric voltage of which is denoted as resting potential, action potential, omega-potential etc. (Dobrin *et al.*, 1979; Adey, 1981). Between the outer surface of the cell membrane and the inner contents of the cell there is always the electric potential difference, which is created because of different concentrations of K^+ , Na^+ and Cl^- inside and outside of the cell and their different permeability through the cell membrane (Kiang *et al.*, 2005). Their value in the human body varies ~50–80 mV, and is defined by the galvanic contact of a voltmeter input with an object that indicates the galvanic type of their source (Cleary, 1993). When excited, a living cell changes the membrane electric potential due to changes in membrane permeability and active ion movement through the membrane. In cells of excitable tissues (muscle, nervous), these processes can occur within a very short time intervals (milliseconds) and are called “current action” potential. Their magnitude makes up ~120 mV. Electromagnetic fields refer to non-ionizing radiation (NIR), e.g. the radiative energy that, instead of producing charged ions when passing through matter, has sufficient energy only for excitation. Nevertheless it is known to cause biological effects (Kwan-Hoong, 2003). The NIR spectrum is divided into two main regions, optical radiations and electromagnetic fields. The optical spectrum can be further sub-divided into ultraviolet, visible, and infra-red. The electromagnetic fields are further divided into radiofrequency (microwave, very high frequency and low frequency radio wave). NIR encompasses the long wavelength (> 100 nm) and low photon energy (<12.4 eV) portion of the electromagnetic spectrum, from 1 Hz to $3 \cdot 10^{15}$ Hz. Research carried out in the 1990ies and subsequent years established the property of animal and plant tissues to

generate relatively strong transient NIR electric fields due to mechanical stresses and temperature changes in biological structure (Anderson, 1993). These electric fields are mainly due to the piezoelectric and pyroelectric voltage electric polarization of natural biological structures. Owing to cell metabolism, electric dipoles (polar and ionized molecules) involved in polarization of biostructures are continuously destroyed and restored, i.e. this is a non-equilibrium polarization (Barnes & Greenebaum, 2006). Such type of non-equilibrium electric polarization is known as a main characteristic of electrets (Gubkin, 1978). Electrets include dielectric insulators and semiconductors, which, under certain conditions, e.g. under the influence of a strong electrostatic field or ionizing radiation, light and other factors, acquire the property to generate an external electric field, existing for a long time (days, years) and slowly diminish due to the destruction of their substance by polarization (Sessler & Gerhard-Mulhaupt, 1998). Along with the electromagnetic field, electrets generate specific electric currents produced by heating – thermally stimulated current (TSC) (Gross, 1964). Electrets belonging to the non-galvanic type of electrical sources tend to a strong electric field (up to 10^6 V/m) and to the infinitesimal electric current ($\sim 10^{-14}$ A/mm²). By analogy with the physical fields, the electric field emitted from the human body and its physical alterations resemble the electric field generated by electrets. The electrets play an important role in the functioning of many biological structures as they themselves possess electret properties. The bioelectret fields registered on the surface of the human body are basically generated by the basal cells of the epidermis (Marino, 1988). Dermis cells adjacent to the bottom layer of basal cells are surrounded by a conductive interstitial fluid whose electric voltage while grounding on the human body is close to zero (so called ground potential). This interstitial fluid screens off electromagnetic fields of underlying tissues. With the average thickness of the epidermis (~ 0.1 mm) and the maximum value of electric voltage (~ 30.0 V), the electric field strength can reach significant values at ~ 300000 V/m (Seto et al., 1992). The strength of the electric field is quite sufficient for its influence on the biological processes in cells and surrounding tissues, including the synthesis of proteins and nucleic acids (Liboff *et al.*, 1984; Frey, 1993; Shimizu *et al.*, 1995). This electric field along with the field of transmembrane asymmetry of ions concentrated at the inside and outside of the membrane ($\sim 10^5$ V/cm²) can participate in the cooperative effects in cell membrane structures (Holzel & Lamprecht, 1994; Miller, 1986). Thus, owing to the bioelectret condition of certain subcellular structures in the cell and its surroundings a slowly oscillating electric field is generated that is strong enough to influence the biological processes. This field and the electric field due to the piezoelectric voltage and intramembrane electric field form the total electromagnetic field of the cell and its supracellular structures. It is known that the human skin emanates electromagnetic waves in close ultraviolet range, optic range and also in close infrared range. Infrared thermal bioradiation is found in the middle infrared range at wavelengths from 8 to 14 μ m. At a wavelength of 9.7 μ m infrared bioradiation has its maximum value at $t = 36.6$ °C. At this temperature the skin emission is closest to the emission of an absolute black body (ABB) having the same temperature. Infrared emission penetrates the skin surface at a depth of ~ 0.1 mm, and is reflected in accordance with the physical laws of reflection of the visible part of the electromagnetic spectrum. Evidently, radiation energy influences tissues while being absorbed by them. Yu.V. Gulyaev and E. E. Godik (Gulyaev & Godik, 1984) determined that the threshold of skin sensitivity for infrared radiation compiled $\sim 10^{-14}$ W/cm². When thermal influence is applied to the point of threshold skin sensitivity, there develops a physiological reaction toward the thermal flow. The intensity of the radiated thermal flow generated by the skin makes up $\sim 2.6 \cdot 10^{-2}$ W/cm². The second component of electromagnetic waves is bioluminescence (Young & Roper, 1976; Chang *et al.*, 1998). It is supposed that biophotons, or ultraweak photon emissions of biological objects, are weak electromagnetic waves in the optical range of the spectrum (Cohen & Popp, 1997). The typical observed emission of biological tissues in the visible and ultraviolet frequencies ranges from 10^{-19} to 10^{-16} W/cm² ($\sim 1-1000$ photons·cm⁻²·sec⁻¹) (Edwards *et al.*, 1989; Choi *et al.*, 2002). This light intensity is much weaker than the one to be seen in the perceptually visible and well-studied spectrum of normal bioluminescence detectable above the background of thermal radiation emitted by tissues at their normal temperature (Niggli, 1993). Bioelectric emission from parts of the human body like thumbs can be easily detected with the method of Color coronal spectral analysis by applying gas electrical discharge of high voltage and frequency developed by I. Ignatov (Ignatov, 2005). Its advantages include safety, sterility, clarity and interpretability of the data obtained, ease of storage and subsequent computer data processing, the ability to monitor the development of processes in time, comparing the structural, functional and temporal processes, etc. The purpose of this research was the studying of possible biophysical methods and approaches for registering various NIR wave's types emitted

from the human body (electromagnetic waves, infrared radiation, thermo radiation) and methods of their visualization by different techniques including magnetography, infrared thermography, chemiluminescence and coronal gas discharge spectral analysis.

2. Materials and methods

2.1. Infrared thermography (IRT)

The research was made using infrared thermography (IRT) method according to M. Marinov. The range of the infrared thermal-imaging camera was in the middle infrared range from 9 μm to 14 μm . The temperature range was from 24.0 $^{\circ}\text{C}$ to 38.0 $^{\circ}\text{C}$. The first camera was Inframetrics/FLIR ThermaCam PM 290 wave type. FLIR ThermaCam PM 290, FLIR 390, Inframetrics PM 250 and Inframetrics PM 350 thermal infrared cameras were of FLIR short wave type, handheld, Focal Plane Array cameras are capable of temperature measurement. These cameras stored images on a PCMCIA Card, and the images were further analyzed using one of several available FLIR software packages (Thermogram 95, FLIR Reporter 2000 Software, Researcher 2000). The second camera (D.I.T.I.) was a totally non-invasive clinical imaging camera for detecting and monitoring a number of diseases and physical injuries, by revealing the thermal abnormalities present in the human body's patterns. It was used as a tool for diagnosis and prognosis, as well as monitoring therapy progress; the type of this device was TB 04 K.

2.2. Registration of electromagnetic fields

The registration of electromagnetic fields was used with super conductive detectors based on Joseffson junctions – device made by sandwiching a thin layer of insulating nonsuperconducting material between two layers of superconducting cooper pairs (S-I-S). This allows the registering of magnetic fields 10^{10} times weaker than the Earth's magnetic field. The study of electric field emitted by the human body was done using a standard Faraday cage formed by conducting material (aluminum foil) blocks with external static and non-static electric fields by channeling electricity through the conducting material, providing constant voltage on all sides of the enclosure.

2.3. NES and DNES experiments on interaction of electromagnetic field with water

The research was made with the method of Non-equilibrium spectrum (NES) and Differential non-equilibrium spectrum (DNES). The device measures the angle of evaporation of water drops from 72° to 0° . As the main estimation criterion was used the average energy ($\Delta E_{\text{H...O}}$) of hydrogen O...H-bonds between H_2O molecules in water's samples. The spectrum of water was measured in the range of energy of hydrogen bonds 0.08–0.1387 eV or 8.9–13.8 μm with a specially designed computer program.

3. Results and discussion

3.1. Electric fields

The electric field surrounding the human body with frequency $\nu = 1 \cdot 10^3$ Hz is created by electrochemical processes in the organism and is modulated by the rhythm of internal organs (Gulyev, Godik, 1984). The spatial distribution of the electric field around the body reflects the teamwork of the different organs and systems in the organism. There are also electric fields, which are generated by accumulation of triboelectric (caused by friction) charge on the epidermis, which depends on epidermal electric resistance and varies from 10^9 to 10^{11} Ω/cm^2 . Radiothermal emission is being detected in the centimeter and decimeter range of

the spectrum. This type of emission is connected with the temperature and the biorhythms of the internal organs, and is being absorbed by the surface skin layer at a depth from 5 cm to 10 cm (Gulyaev & Godik, 1984). Long persistent electric field emitted from the human body can be detected with an electrometer voltmeter after neutralizing electric charges on the skin caused by triboelectric charges. The electric strength of this field is undergoing slow oscillations, and most patients exert its value within the range of 100–1000 V/m at a distance of 5–10 cm from the body. People in a state of clinical death usually have the electric field strength's value reduced to 10–20 V/m after 2–3 hours of cardiac arrest. Intensity vector of the detected electric field is found to be normal at the surface of the skin, and the electric voltage is inversely proportional to the distance. On the skin surface the electric voltage of the field (the difference of its electric potential with respect to ground potential) reaches essential values of ~10000 mV or more, i.e., is about 1000 times greater than the source electric voltage of the electric unit above the bioelectric potentials. This allows us to characterize the electric field detected from the human body as relatively strong electric field emitted from living tissues. Its electric voltage was measured by electrometric methods, identified by a non-galvanic type of its source. If the physical basis of the generation of a relatively strong electric field in the human tissue is non-equilibrium electric polarization of the substance due to metabolic processes, the electric field strength should depend on these processes. As noted above, this dependence is actually observed: inhibition of tissue metabolism due to hypoxia during cardiac arrest was accompanied by drop in the electric field strength. This relationship is confirmed in experiments on animals (Gerald et al., 2008). For example, in rats inhibition of metabolism of the tissue due to cardiac arrest (death of the animal) or by general anesthesia is accompanied by a significant drop in the electric field strength (Bars & Andre, 1976). Electric fields depend on the magnitude of the electric voltage and the distance from the source (Kwan-Hoong, 2003). Generally, the electric voltages are stable and remain the same; however electric fields are easily perturbed and distorted by many surrounding objects. Relatively strong electric field investigated in humans and animals is being formed evidently by the skin's biostructures, since the electric fields of the underlying tissues are largely shielded by conductive interstitial fluid (Goodman *et al.*, 1995; Gulyaev & Godik, 1990). The basal cells of the epidermis – the top layer of the skin, contribute the most to the detected electric field. Electric polarization vector of these cells is normal to the surface of the skin, i.e., coincides with the electric voltage's vector field, and yet it is inherent in the metabolism intensity, conditioning the generation of the electric field.

3.2. Magnetic fields

Magnetic field of a living organism can be caused by three reasons. First of all, it is ion channels arising from the electrical activity of cell membranes (primarily muscle and nervous cells). Another source of magnetic fields are the tiny ferromagnetic particles, trapped or specially introduced into the human body. These two sources create their own magnetic fields. In addition, at imposition of external magnetic field there appears inhomogeneity of the magnetic susceptibility of different organs and tissues distorting the external magnetic field (Wikswa & Barach, 1980). The magnetic field in the last two cases is not accompanied by the appearance of the electric field, so the study of the behavior of magnetic particles in the human body and the magnetic properties of various organs are applicable only with magnetometric methods. Biocurrents, on the contrary, except for the magnetic fields, create the distribution of electric potentials on a body's surface. Registration of these electric potentials has long been used in research and clinical diagnostics – in electrocardiography, electroencephalography, etc (Cohen, 1968). It would seem that their magnetic counterparts, i.e. magnetocardiography and magnetoencephalography recording the signals from the same electrical processes in the body, will give almost the same information about the studied organs. However, as follows from the theory of electromagnetism, the structure of the electric current source in the electric conductive medium (the body) and the heterogeneity of the medium have significantly different impact on the distribution of magnetic and electric fields: some types of bioelectric activity manifest themselves primarily in the electric field, giving a weak magnetic signal, while others – on the contrary, create a rather strong magnetic signal (Zhadin, 2001; Anosov & Trukhan, 2003). Therefore, there are many biophysical processes whose observation is preferable by magnetographic methods. Magnetography does not require direct contact with the investigated object, i.e., it allows carrying out measurements over a bandage or other obstructions. It is not only practically useful for diagnostics, but has

a fundamental advantage over electrical methods towards data recording, as the attachment of the electrodes on the skin can be a source of slowly varying contact electric potentials. There are no such spurious noises while using magnetographic methods, therefore, magnetography allows, in particular, to reliably explore slowly occurring processes (with the characteristic time of tens of minutes). Magnetic fields rapidly diminish with distance from the source of the activity, as they are caused by relatively strong currents running in the body, while the surface potentials are determined mainly by the weaker and “smeared” electric currents in the skin. Therefore, magnetography is more convenient for accurate determination (localization) of bioelectric activity parts on the human body. And finally, the magnetic field vector is characterized not only by the absolute value but also by the direction, which also may provide additional useful information. However, it should not be assumed that the electricity and magnetographic methods compete with each other. On the contrary, it is their combination that gives the most complete information about the processes being investigated. But for each of the individual methods, there are practical areas wherein the use of any one of them is preferable. Water is the main substance of all living organisms and the magnetic field exerts a certain influence on water. This influence is a complex multivariate influence, which the magnetic field exerts on dissolved in water metal cations (Fe^{2+} , Fe^{3+}) and the structure of the hydrates and water associates (Mosin, 2011). It was experimentally proved that the magnetic field acts much weaker on still unmoved water, because water has a conductivity; as water moves in the electromagnetic field, a small electric current is generated (Mosin, 2012). The research performed with superconductive detectors based on Josephson junctions shows that magnetic fields around the human body are in the range from 1 to 100 Hz. The magnetic activity of the brain for example makes up $\sim 30 \cdot 10^{15}$ T/Hz^{1/2}. The magnetometric system has a sensitivity of $10 \cdot 10^{15}$ T/Hz^{1/2} in the range of 1 to 100 Hz (Gulyaev & Godik, 1990).

3.3. NES and DNES analysis of water

Water seems to be a good model system for studying the interaction with electromagnetic fields and structural research. Recent data indicated that water is a complex associated non-equilibrium liquid consisting of associative groups (clusters) containing from 3 to 50 individual H₂O molecules (Keutsch & Saykally, 2011). These associates can be described as unstable groups (dimers, trimers, tetramers, pentamers, hexamers etc.) in which individual H₂O molecules are linked by van der Waals forces, dipole-dipole and other charge-transfer interactions, including hydrogen bonding (Ignatov & Mosin, 2013c). At room temperature, the degree of association of H₂O molecules may vary from 2 to 21. The measurements were performed with NES and DNES methods. It was established experimentally that in the process of evaporation of water drops, the wetting angle θ decreases discreetly to 0, and the diameter of water drop basis is only slightly altered, that is a new physical effect (Antonov & Yuskesseliya, 1983). Based on this effect, by means of measurement of the wetting angle within equal intervals of time is determined the function of distribution of H₂O molecules according to the value of $f(\theta)$. The distribution function is denoted as the energy spectrum of the water state. A theoretical research established the dependence between the surface tension of water and the energy of hydrogen bonds among individual H₂O-molecules (Antonov, 1995). The hydrogen bonding results from interaction between electron-deficient H-atom of one H₂O molecule (hydrogen donor) and unshared electron pair of an electronegative O-atom (hydrogen acceptor) on the neighboring H₂O molecule; the structure of hydrogen bonding may be defined as $\text{O} \cdots \text{H}^{\text{nt}} - \text{O}^{\text{n}}$. For calculation of the function $f(E)$ represented the energy spectrum of water, the experimental dependence between the wetting angle (θ) and the energy of hydrogen bonds (E) is established:

$$f(E) = b \times f(\theta) / (1 + b \times E)^2 \quad (1)$$

$$\text{where } b = 14.33 \text{ eV}^{-1} \quad (2)$$

The relation between the wetting angle (θ) and the energy (E) of the hydrogen bonds between H₂O molecules is calculated by the formula:

$$\theta = \arcsin(-1 - 14.33E) \quad (3)$$

The energy spectrum of water is characterized by a non-equilibrium process of water droplets evaporation, therefore, the term non-equilibrium spectrum (NES) of water is used. The energy of hydrogen bonds measured by NES is determined as $\bar{E} = -0,1067 \pm 0,0011$ eV.

The difference $\Delta f(E) = f(\text{samples of water}) - f(\text{control sample of water})$

– is called the “differential non-equilibrium energy spectrum of water” (DNES).

Thus, DNES spectrum is an indicator of structural changes of water as a result of various external factors. The cumulative effect of these factors is not the same for the control sample of water and the water sample being under the influence of this factor. Fig. 1 shows NES-spectrum of deionized water that was used as a model system for studying the interaction of electromagnetic field with water. On the X-axis are given three scales. The energies of hydrogen bonds among H₂O molecules are calculated in eV. On the Y-axis is shown the energy distribution function $f(E)$ of H₂O molecules measured in eV^{-1} . It was shown that the window of transparency of the earth atmosphere for the electromagnetic radiation in the middle IR-range almost covers NES-spectrum of water. Arrows A and B designate the energy of hydrogen bonds among H₂O molecules. Arrow C designates the energy at which the human body behaves itself as absolute black body (ABB) at optimum temperature 36.6 °C and adsorbs the thermal radiation. A horizontal arrow designates the window of transparency of the earth atmosphere for the electromagnetic radiation in the middle IR-range.

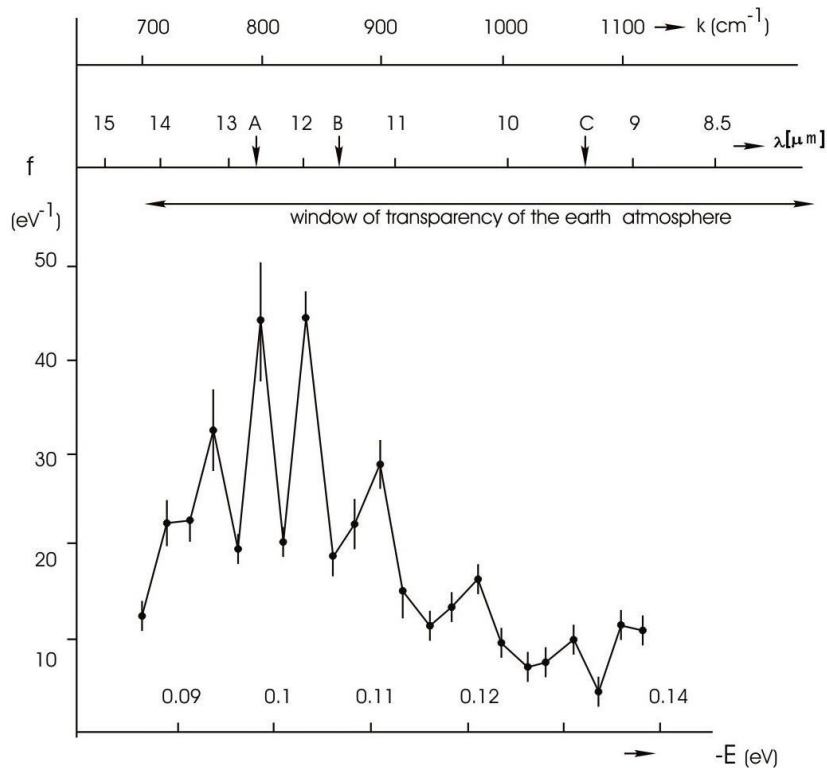


Fig. 1. Non-equilibrium energy spectrum (NES) of water as a result of measurement for 1 year: λ – wavelength, k – wave number.

Another important physical parameter was calculated with NES and DNES methods – the average energy ($\Delta E_{\text{H...O}}$) of H...O-bonds between H₂O compiled -0.1067 ± 0.0011 eV. The most remarkable peculiarity of H...O-bond consists in its relatively low strength; it is 5–10 times weaker than chemical covalent bond. In respect of energy hydrogen bond has an intermediate position between covalent bonds and intermolecular van der Waals forces, based on dipole-dipole interactions, holding the neutral molecules together in gasses

or liquefied or solidified gasses. Hydrogen bonding produces interatomic distances shorter than the sum of van der Waals radii, and usually involves a limited number of interaction partners. These characteristics become more substantial when acceptors bind H atoms from more electronegative donors. Hydrogen bonds hold H₂O molecules on 15 % closer than if water was a simple liquid with van der Waals interactions. The hydrogen bond energy compiles 5–10 kcal/mole, while the energy of covalent O–H-bonds in H₂O molecule – 109 kcal/mole. With fluctuations of water temperature the average energy of hydrogen H...O-bonds in H₂O molecule associates changes. That is why hydrogen bonds in liquid state are relatively weak and unstable: it is thought that they can easily form and disappear as the result of temperature fluctuations. The next conclusion that can be drawn from our research is that there is the distribution of energies among individual H₂O molecules. Further we performed two types of temperature-dependent experiments on heat exchange from the surface of the human body by DNES-method. In the first experiment we studied heat exchange when the temperature of the human body was higher than the temperature of the surrounding environment (curve 1a and 1b on Fig. 2). In the second experiment there was heat exchange when the temperature of the human body was lower than that of the surrounding environment (curve 2a and 2b on Fig. 2). In both experiments a local maximum was detected at 9.7 μm on curve 1 and curve 2 (Fig. 2). This local maximum corresponds to the maximal level of heat emission from the surface of the human body and lays within the “transparency window” of the Earth atmosphere to electromagnetic radiation in the mid IR-range of the electromagnetic spectrum. In this range, the electromagnetic radiation emitted by the Earth in the surrounding space is being absorbed by the Earth atmosphere. There is a statistical difference between the results of heat emission from the surface of the human body to the surrounding environment and back to the human body according to the *t*-criterion of Student at $p < 0.01$. The local maximum on curve 1a is detected at 7.3 eV⁻¹, while the local maximum on curve 2a – at 2.4 eV⁻¹ (Fig. 2).

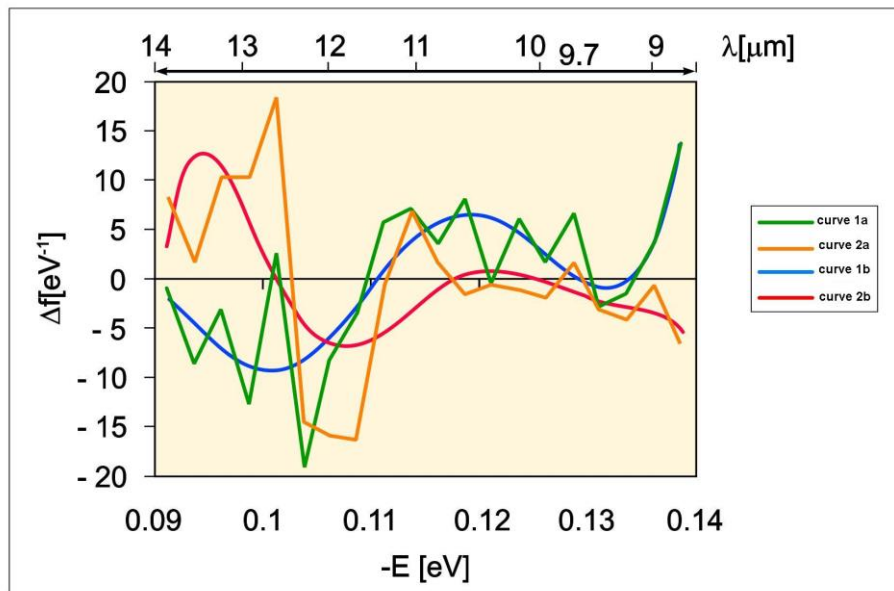


Fig. 2. Differential non-equilibrium energy spectrum (DNES) reflecting the heat exchange of the human body with the surrounding environment.

3.4. Infrared thermography (IRT)

The human body as a biological body has an average temperature in the range from 36.6 to 36.8 °C, The main part of this radiation predominantly falls on human skin with a middle infrared range from 8 to 14 μm. Maximum of spectral density covers the range approx. ~10 μm i.e. the middle wavelength IR range. The physical essence of the thermal radiation consists in the presence of charged particles (electrons and ions), which are in random motion and have the properties of electrical or magnetic polarity. Infrared radiation is

emitted or absorbed by excited atoms or ions when they change their rotational-vibrational movements. Electromagnetic waves propagate throughout the body and reach the surface, passing through the skin and partly emitted into the environment. The intensity of these processes is proportional to the body temperature. The wavelength of infrared radiation emitted by the body depends on the heating temperature: the higher the temperature, the shorter is the wavelength and therefore the higher the emission intensity. Studies have shown that in the long wavelength infrared range (8–14 μm) the human skin radiates as a black body, regardless of age, degree of pigmentation and other features. Therefore, the emissivity of the human skin can be considered equal to 1 absolute unit. In practice, it is proved that the difference between the emission characteristics of the human skin and blackbody still exist, however, it is small and depends essentially on the influence of the surrounding background. The limit of effective temperature measurement is equal to the thickness of the emitting layer (skin layer) and is defined as the distance at which electromagnetic waves propagate from the object's surface before the layer in which the intensity decreases in ~ 2.5 times. Under equal conditions, the greater the wavelength, the greater the depth, which can detect the temperature perturbations. The maximum intensity of thermal radiation at normal ambient temperature is located in the infrared range of the spectrum (wavelength $\sim 10 \mu\text{m}$ at $t = 36.6 \text{ }^\circ\text{C}$). The threshold of skin sensitivity according to Yu.V. Gulyaev and E.E. Godik compile $\sim 10^{-14} \text{ W/cm}^2$ (Gulyaev & Godik, 1990). This led to the feasibility of establishing IR thermal imaging (thermography) for the study of the temperature anomalies. However, the measurement of the thermal radiation of the human body in the IR range gives the true temperature for only the top layer of skin with thickness of $\sim 1 \text{ mm}$; after that the thermal radiation is reflected back into the environment. The temperature of the underlying tissues and organs can be judged indirectly when the temperature changes are “projected” on the skin. Infrared thermography is a scientific method for registering the thermogram – infrared image showing the distribution pattern of infrared waves emitted from the objects (Ring & Hughes, 1986). Thermographic cameras detect radiation in the infrared range of the electromagnetic spectrum (approx. $\sim 0.9\text{--}14 \mu\text{m}$), and on its basis are obtained thermographic images (thermograms) allowing to determine the locations of patterns having different temperatures. Thermograms therefore are actually visual displays of the amount of infrared energy emitted, transmitted, and reflected from the surface of the object. Since infrared radiation is emitted by all objects with the temperature according to Planck's formula for black body radiation, thermography allows to “see” the environment with or without visible illumination. The intensity of the thermal radiation of the body increases with the temperature, therefore thermography allows to see the temperature distribution on the surface of the body. As a result, warm objects are seen better on the cooler environment background; mammals and warm-blooded animals are better visible on the environment. That is why thermography may find many diagnostic applications and is often being used for breast diagnostics, tumor detection etc. Most thermographic cameras use CCD and CMOS image sensors having most of their spectral sensitivity in the visible light wavelength range. The most commonly used is a matrix of indium antimonide (InSb), gallium arsenide (GaAs), mercury telluride (HgTe), indium (In) and cadmium (Cd). The latest technology allows the use of the inexpensive uncooled microbolometer sensors. Their resolution is varied from 160×120 or 320×240 up to 768×1024 pixels in the most advanced camera models. Often the thermogram reveals temperature variations so clearly that a photograph is not necessary for further analysis. Usually a block of the focal planes of thermo images can detect radiation in the medium (3 to 5 μm) and long (8 to 15 μm) infrared wave band, designated as MWIR and LWIR corresponding to two infrared windows with high coefficient of transmittance. Improperly selected temperature range on the surface of the objects, indicates a potential problem.

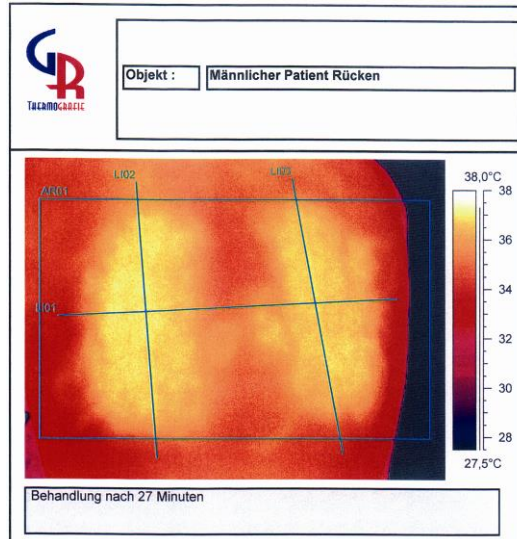


Fig. 3. Thermovisual snapshot of the result of bioinfluence of Ch. Drossinakis on skin section of the back of a person suffering from radiculitis after 27 min

It should be noted that the intensity of the thermal radiation of the human body in the microwave (MW) range is much smaller in magnitude than in the infrared part of the spectrum (Sisodia, 2007). In particular at a wavelength of 17 cm the intensity is less in ~ 10 times, so the heat reception signals in this range of the spectrum require equipment with higher sensitivity. However, the advantage of this method is that the measurement range and the depth of radiation penetration is much greater, therefore it is possible to obtain data on the temperature parameters of the internal organs and structures of the human body, but the resolution is significantly reduced, therefore it is impossible to obtain reliable thermal image of the study area. Infrared thermography registered a thermal infrared radiation emitted by the capillary network of the skin, which is used in medicine for thermovisual diagnostics. The closer an ailing organ is to the skin, the more accurate the diagnosis based on a thermal signal. Today it seems to be an established fact that some people possess the ability to increase the temperature of the treated area of the human body. Figure 3 shows the thermovisual result of the temperature difference between the initial ($t = 35.6^{\circ}\text{C}$) and final skin section temperature ($t = 37.3^{\circ}\text{C}$) of the person before and after the treatment of Drossinakis. It was calculated that the temperature of the skin part was increased after the treatment on 1.7°C . In this connection there should be noted two important empirical thermography results obtained by M. Marinov (Marinov & Ignatov, 2008), which allow the medical diagnostics of various human organs and monitoring of their condition and malfunction by this method. Fig. 4a shows the thermography snapshot of a patient having a benign tumour growth in the mammary gland, which has a higher temperature than the surrounding tissues' lower temperature with 0.54°C . Fig. 4b shows a patient having hyperfunction of thyroid gland, which has higher temperature than the surrounding tissues' lower temperature at 0.76°C . The middle value on the scale is 36.6°C . In the left side of the scale there are temperatures less than 36.6°C . In the right side of the scale there are temperatures more than 36.6°C .

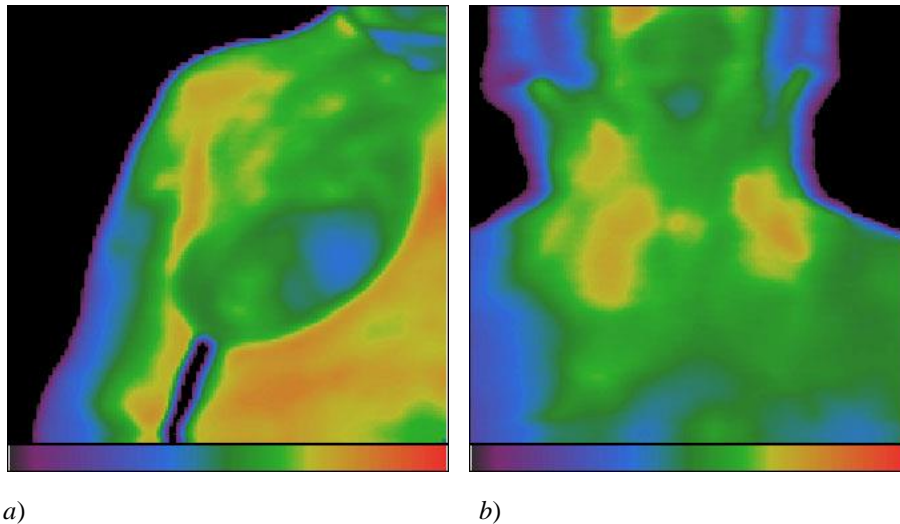


Fig. 4. Thermovisual snapshots of the human body (Marinov, 2008): *a*) – patient having a benign tumor growth in the mammary gland; *b*) – patient having hyperfunction of thyroid gland

4. Conclusions

The approaches and methods for detecting of infrared thermal flow, electric and magnetic fields were presented of applied science and medical diagnostics. With methods as NES and DNES may be applied for studying the interaction of electromagnetic fields with water and structural studies.

Acknowledgements

The authors are thankful to Vassil Marinov from 22nd Clinical and Diagnostical Medical Center, Sofia, Bulgaria for clinical data with thermo camera. The authors are thankful to assistant Lara Weigmann.

References

- Adey, W.R. (1981) Tissue interaction with non-ionizing electromagnetic fields. *Physiol. Rev.*, **61**: 435–514.
- Anderson, L.E. (1993) Biological effect of extremely low frequency electromagnetic fields: *in vivo* studies. *Am. Ind. Hyg. Assoc. J.*, **54**: 186–196.
- Anosov V.N. & Trukhan E.M. (2003) A new approach to the problem of weak magnetic fields: An effect on living objects. *Doklady Biochemistry and Biophysics*, **392**(1-6): 274-278.
- Antonov, A. & Yuskesseliya, L. (1985) Selective high frequency discharge (Kirlian effect). *Acta Hydrophysica*, Berlin, **5**: 29.
- Antonov, A. (1995) Research of the non-equilibrium processes in the area in allocated systems. Dissertation thesis “Doctor of physical sciences”, Blagoevgrad, Sofia.
- Barnes, F.S. & Greenebaum, B. (eds.) (2006) CRC Handbook on biological effects of electromagnetic fields. 3d Edition, Boca Raton: CRC Press, November 2006, Vol. 2, 960 p.
- Bars, Le. & Andre, G. (1976) Biological effects of electric fields on rats and rabbits. *Red. Gen. Elect.* (special issue), July 1976: 91–97.
- Cleary, S.F. (1993) A review of *in vitro* studies: low-frequency electromagnetic fields. *J. Am. Ind. Hyg. Assoc.*, **54**(4): 178–185.
- Cohen, D. (1968) Magnetoencephalography: evidence of magnetic fields produced bi alpha-rhythm currents. *Science*, **161**(3843): 784–786.
- Dobrin, R., Kirsch, C., Kirsch, S. et al. (1979) Experimental measurements of the human energy field. In S.

- Krippner (ed.), *Psychoenergetic Systems: The Interface of Consciousness, Energy and Matter*. New York, Gordon & Breach, 230 p.
- Edwards, R., Ibison, M.C., Jessel-Kenyon, J. & Taylor, R.B. (1989) Light emission from the human body. *Complement Med. Res.*, **3**:16.
- Esterbauer, H., Zollner, H. & Schaur, R. J. (1990) Aldehydes formed by lipid peroxidation: mechanisms of formation, occurrence, and determination. In *Membrane Lipid Oxidation*. Boca Raton, CRC Press, 283 p.
- Frey, A.H. (1993) Electromagnetic field interactions with biological systems. *FASEB Journal*, **7**(2): 272–281.
- Gerardi, G., De Ninno A., Prosdocimi, M. *et al.* (2008) Effects of electromagnetic fields of low frequency and low intensity on rat metabolism. *Biomagnetic Research and Technology*, **6**: 3.
- Gubkin, A.N. (1978) *Electrets*. Moscow, Nauka. 192 p.
- Gross, B. (1964) *Charge storage in solid dielectrics; a bibliographical review on the electret and related effects*. New York, Elsevier Pub. Co., 230 p.
- Goodman, R., Greenbaum, B. & Marron, M.T. (1995) Effects of electromagnetic fields on molecules and cells. *Int. Rev. Cytol.*, **158**: 279–338.
- Gulyaev, Yu.V. & Godik, E.E. (1984) On the possibilities of the functional diagnostics of the biological subjects via their temporal dynamics of the infrared images. *USSR Academy Nauk Proceedings/Biophysics*, **277**: 1486–1491.
- Gulyaev, Yu.V. & Godik, E.E. (1990) Human and animal physical fields. *Scientific American*, **5**: 74–83.
- Gulyaev, Yu.V. & Godik, E.E. (1991) Functional Imaging of the Human Body. *IEEE Engineering in Medicine and Biology*, **10**: 21–29.
- Holzel, R. & Lamprecht, I. (1994) Wirkungen elektromagnetischer Felder auf biologische Systeme. *Nachrichtentech Elektron*, **44**(2): 28–32.
- Ignatov, I., Antonov, A. & Galabova, T. (1998) *Medical Biophysics – Biophysical Fields of Man*. Gea Libris, Sofia: 1–71.
- Ignatov, I., Antonov, A. & Galabova, T. (2002) Scientific Research Studies with Christos Drossinakis (October 2001 – October 2002), *Int. Conference “Man and Nature”*, SRCMB, Sofia.
- Ignatov, I. (2005) *Energy Biomedicine*, Gea-Libris, Sofia, 1–88.
- Ignatov, I. (2010) Which Water is Optimal for the Origin (Generation) of Life? *Euromedica*, Hanover: 34-37.
- Ignatov, I., Tsvetkova, V. (2011) Water for the Origin of Life and “Informationability” of Water, Kirlian (Electric Images) of Different Types of Water, *Euromedica*: 62-65.
- Ignatov, I. (2011) Entropy and time in living matter, *Euromedica*: 74.
- Ignatov, I., Mosin, O. V. & Naneva, K. (2012) Water in the Human Body is Information Bearer about Longevity, *Euromedica*, Hanover: 110-111.
- Ignatov I. (2012) Conference on the Physics, Chemistry and Biology of Water, Water in the Human Body is Information Bearer about Longevity, NY: *Vermont Photonics*.
- Ignatov, I. & Mosin, O.V. (2012) Kirlian effect in biomedical diagnostics and study of bioenergetical properties of biological objects and water. *Biomedical Radio electronics, Biomedical Technologies and Radio Electronics*, **12**: 13–21 [in Russian].
- Ignatov, I. & Mosin, O.V. (2013a) Method for Color coronal (Kirlian) spectral analysis. *Biomedical Radio electronics, Biomedical Technologies and Radio Electronics*, **1**: 38–47 [in Russian].
- Ignatov, I. & Mosin O.V. (2013b) Color crown spectral Kirlian analysis in the modeling of non-equilibrium conditions with a gas electric discharge that simulates the primary atmosphere. *Nano engineering*, **12** (30): 3–13 [in Russian].
- Ignatov, I. & Mosin, O.V. (2013c) Structural mathematical models describing water clusters. *Journal of Mathematical Theory and Modeling*, **3** (11): 72–87.
- Ignatov I., Mosin O.V. (2013) Possible Processes for Origin of Life and Living Matter with modeling of Physiological Processes of Bacterium *Bacillus Subtilis* in Heavy Water as Model System, *Journal of Natural Sciences Research*, **3** (9): 65-76.
- Ignatov, I., Mosin, O. V. (2013) Modeling of Possible Processes for Origin of Life and Living Matter in Hot Mineral and Seawater with Deuterium, *Journal of Environment and Earth Science*, **3**(14): 103-118.
- Ignatov, I. & Mosin, O.V. (2014) Color Coronal (Kirlian) Spectral Analysis in Modeling of Nonequilibrium Conditions with the Gas Electric Discharges, Simulating Primary Atmosphere, *Biomedical*

Radioelectronics, **2**: 42-51. [in Russian]

Ignatov, I., Mosin, O.V. (2014) Photoreceptors in Visual Perception and Additive Color Mixing. Bacteriorhodopsin in Nano- and Biotechnologies, *Advances in Physics Theories and Applications*, **27** :20-37.

Ignatov, I., Mosin, O.V., Velikov, B., Bauer, E. & Tyminski, G. (2014) Longevity Factors and Mountain Water as a Factor. Research in Mountain and Field Areas in Bulgaria, *Civil and Environmental Research*, **6** (4): 51-60.

Ignatov, I., Mosin, O. V., Niggli, H.&Drossinakis, Ch. (2014) Evaluating Possible Methods and Approaches for Registering of Electromagnetic Waves Emitted from the Human Body, *Advances in Physics Theories and Applications*, **30**: 15-33.

Ignatov, I., Mosin, O. V. (2014) The Structure and Composition of Carbonaceous Fullerene Containing Mineral Shungite and Microporous Crystalline Aluminosilicate Mineral Zeolite. Mathematical Model of Interaction of Shungite and Zeolite with Water Molecules *Advances in Physics Theories and Applications*, **28**: 10-21.

Kirlian, S. D. (1949) Method for receiving photographic pictures of different types of objects. USSR Patent № 106401.

Kiang, J.G., Ives J.A. & Jonas, W.B. (2005) External bioenergy-induced increases in intracellular free calcium concentrations are mediated by Na⁺/Ca²⁺ exchanger and L-type calcium channel. *Mol. Cell Biochem.*, **271**:51.

Kwan-Hoong, Ng. (2003) Non-ionizing radiations – sources, biological effects, emissions and exposures. *Proceedings of the International Conference on Non-Ionizing Radiation at UNITEN (ICNIR2003). Electromagnetic Fields and Our Health*. 20–22 October 2003.

Liboff, A.R., Williams, T., Strong, D.M. & Wistar, R. (1984) Time-varying magnetic fields: effect on DNA synthesis. *Science*, **223**: 818–820.

Marino, A.A (Ed.) (1988) *Modern Bioelectricity*. Maricel Dekker, New York, Basel, ISBN 0-8247-7788-3.

Marinov, M. & Ignatov, I. (2008) Color Kirlian spectral analysis. Color observation with visual analyzer. *Euromedica*, Hanover, 57–59.

Miller, M.W. (1986) Extremely low frequency (ELF) electric fields: experimental work on biological effects. *CRC Handbook of biological effects of electromagnetic fields*, 138–168.

Mosin, O.V. (2011) Magnetic devices for water treatment. *C.O.K. Publishing House “Media Technology” (Moscow)*, **6**: 24–27 [in Russian].

Mosin, O.V. (2012) Advanced technologies and equipment for magnetic water treatment (review). *Water supply and sanitary technique*, **8**: 12–32 [in Russian].

Porter, N.A. & Wujek, D.G. (1988) *Reactive Oxygen Species in Chemistry, Biology, and Medicine*. In A. Quintanilha, Ed. New York, Plenum Press, pp. 55–79.

Ring, E.F.J. & Hughes, H. (1986) Real time video thermography in recent developments in medical and physiological imaging. *Suppl. Journal of Medical Engineering and Technology*, 86–89.

Sessler, G.M. & Gerhard-Multhaupt, R. (eds) (1998) *Electrets*. Laplacian Press, Morgan Hill, California, USA, ISBN 1-885540-07-8.

Seto, A., Kusaka, C., Nakazato, S. et al. (1992) Detection of extraordinary large bio-magnetic field strength from human hand. *Acupuncture Electrother Res. Int. J.*, **17**:75.

Shimizu H., Suzuki, Y. & Okonogi, H. (1995) Biological effects of electromagnetic fields. *Nippon Eiseigaki Zasshi.*, **50**(6): 919–931.

Sisodia, M.L. (2007). *Microwaves: introduction to circuits, devices and antennas*. New Delhy, New Age International Ltd., ISBN 8122413382, 602.

Wiksw, J. & Barach, J. (1980) An estimation of the steady magnetic field strength required to influence nerve condition. *IEEE Trans. Bio-Med. Eng.*, **27**: 722–723.

Young, R.E. & Roper, C.F. (1976) Bioluminescent countershading in midwater animals: evidence from living squid, *Science*, **191**(4231): 1046–1048.

Zhadin, M.N. (2001) Review of russian literature on biological action of DC and low-frequency AC magnetic fields. *Bioelectromagnetics*, **22**: 27– 45.

Zlatkevich, L. & Kamal-Eldin, A. (2005) *Analysis of Lipid Oxidation*. In: A. Kamal-Eldin & J. Pokorn (Eds.). New York, AOCS Publishing, 281 .